A WIRELESS TRANSMISSION MAGNETIC CORE BASED ON ROBUST CHARACTERISTICS

Jiangyong XIONG[1]*, Zhenghao LI[2], Chongchong LI[3], Junhua WU[4]

In this research, we aimed at enhancing the performance of wireless charging for new-energy vehicles by studying the application of magnetic core in wireless charging transmission. The study compared different forms of dynamic electric vehicle charging and investigated the variations of magnetic core coupling coefficient under both static and dynamic wireless charging conditions with misalignment between receiving and transmitting coils. Our findings indicated that Rec-Rec shaped cores exhibited significantly higher coupling coefficients than receiving and transmitting coils when seeking an optimal magnetic couple topology with superior coupling factor. However, when considering misalignment, this topological advantage became less pronounced making it more suitable for static charging applications. These results were validated using tests.

Keywords: wireless charging, magnetic core, topology optimization, coupling coefficient, robust characteristics

1. Introduction

Electric vehicles are a new type of environmentally friendly vehicle powered by on-board power supply. It has the advantages of environmental protection, energy saving, zero emission, low noise, etc. It is an effective strategy to alleviate the large amount of non-renewable energy consumption, environmental pollution and other problems [1]. In recent years, China's electric vehicles have achieved rapid development. Fig. 1 shows the sales volume of pure electric vehicles in China in 2012-2021. The figure illustrates a significant growth in the production of electric vehicles in China, with an output of 11,200 units in 2012 and a remarkable increase to nearly 3 million pure electric vehicles by 2021, representing a staggering surge of 268 times [2]. The charging mode has emerged as the primary bottleneck impeding the robust advancement of electric vehicles accompanying their rapid development.

[1]* Nanjing Vocational College of Information Technology, Nanjing, China, *Corresponding author's email: xiongjy@njcit.cn
[2] Nanjing Automobile (Group) Corporation, Nanjing, China
[3] Nanjing Vocational College of Information Technology, Nanjing, China
[4] Nanjing Forestry University, Nanjing, China

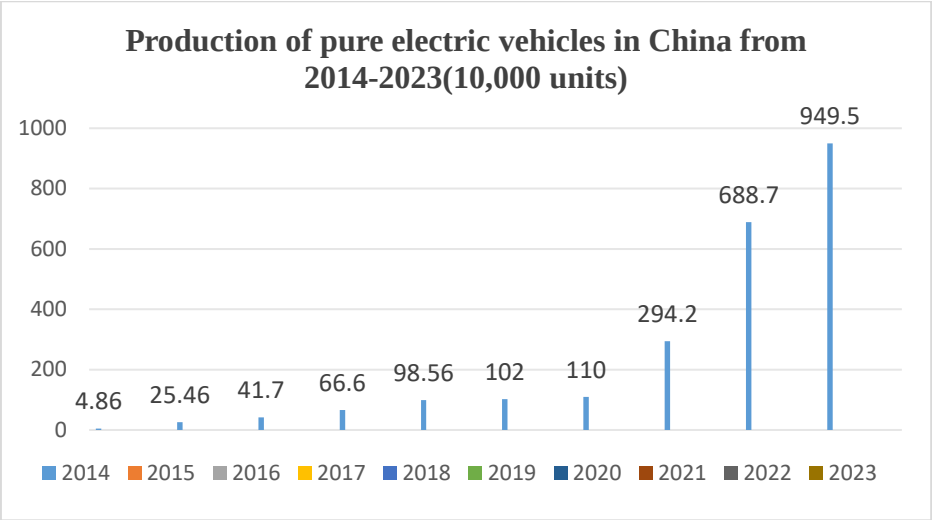

Fig. 1. Production of pure electric vehicles in China from 2014 to 2023 (10,000 units)

2. Background introduction

In the use of electric vehicles, the charging method commonly used in the market is wired charging, that is, the electricity is transmitted from the grid to the on-board energy storage battery by cable. This way requires the charging line connection, the operation is not flexible, cannot achieve automatic control. Secondly, in the process of use, the voltage, current is too high, or the battery overcharge is easy to lead to thermal runaway of the battery, thus causing combustion, and there are great safety risks in rainy days. Compared with the traditional method, Wireless Power Transmission (WPT), a non-physical contact charging method, has the advantages of convenience and safety, and can adapt to the severe external environment and facilitate automatic control [3,4]. In addition, wireless charging is faster than the traditional charging line connection charging method, eliminating a large number of charging piles and charging stations and making it more energy efficient. Using wireless charging to power electric vehicles is the future trend [5]. The WPT devices for pure electric vehicles must be highly efficient, and the magnetic core near the transmitting and receiving coils should be as tiny as feasible to reduce cost and size. A rod and shaped core with a double-sided winding coil is proposed for this WPT device [6].

In contrast to conventional parameter optimization methods, we achieve the optimal shape [7] through topological optimization without introducing any design parameters. The on/off method based on normalized Gaussian networks (NGnet) is particularly valuable for constructing rotating machines and antennas [8]. We successfully address two-dimensional optimization challenges using our proposed strategy. In this study, we extend this approach to a 3D optimization design for a magnetic core of a WPT device with a double-sided winding coil. The core form is

adjusted in this optimization process to enhance the coupling coefficient of the WPT device. Additionally, due to the inherent challenge of preventing dislocation between the transmit coil and receiving coil, we must develop robust WPT devices [9-13].

3. Optimization method

The material properties within the design region are determined by the value of the defined form function while optimizing WPT device topology using NGnet.

$$\mathrm{y}(x)=\sum_{i=1}^{\mathrm{n}}\lambda_i \mathrm{a}_i(x) \tag{1}$$

The symbols i, λ ,x , and n represent the weighting coefficient, index of centers, position variable, and number of Gaussian functions in the finite element method respectively. The function ai i (x) denotes the normalized Gaussian function.

$$\mathrm{a}_i(x)=M_i(x)/\sum_{j=1}^{\mathrm{n}}M_j(x) \tag{2}$$

$$Mi\ (\mathrm{x})=\frac{1}{\sqrt{(2\pi)^3\sigma^3}}\exp\left\{-2\sigma^{-2}\left|x-x_i\right|^2\right\} \tag{3}$$

The standard deviation of the value is assigned to M as 21.0 mm, and xi represents the Gaussian M center i (x). The form function y (x) determines the finite element c in the Material Property Cc design area according to the following equation.

$$C\mathrm{c}=\begin{cases}Ferrite & \mathrm{y}(x)\geq 0\\ Air & \mathrm{y}(x)<0\end{cases} \tag{4}$$

The magneto static equation below is ultimately solved to ascertain the objective function.

$$rotR_m(rotU)=J \tag{5}$$

The magnetic resistance, vector potential, and current density are represented by R_m, U, and J respectively in equation (5).

$$\sum_{\mathrm{j}}U_j\int_{\Omega}rot\mathrm{n}_i R_{\mathrm{m}}\left(rot\mathrm{n}j\right)d\Omega=\int_{\Omega coil}\mathrm{n}i\cdot Jd\Omega \tag{6}$$

The vector interpolation function Ni is utilized in the NGnet based on/off method to determine the magnetic resistivity in equation (6), as specified by equation (4).

In the process of optimization, the objective function is maximized using microgenetic algorithm (μ GA) constraints. This reduces topology optimization to determining an array of real numbers denoted as λ.

4. Optimize the problem

We aimed to optimize the core shape in order to maximize the efficiency of the wireless power transfer (WPT) device, while minimizing its size and cost. Additionally, we strived to maintain high efficiency even in cases of misalignment between the transmitting and receiving coils. Therefore, our objective was to achieve an optimal core shape that could effectively withstand deviations by maximizing magnetic coupling across various vertical deviation modes. The optimization problems were formulated considering robustness.

$$\max_{\omega} F(\omega), F(\omega) = \frac{1}{N_p}\sum_{i=1}^{N_p} k_i(\omega), \qquad sub.to\ \Omega_M \le \frac{\Omega_D}{2} \tag{7}$$

The coupling coefficients ki(ω) (i = 1, 2,... , Np), represent the coupling strength of each dislocation mode, while V represents the total volume of the magnetic core and Vd represents the volume of the design area. In problem (7), we simplify by considering the average value of these coefficients, but it is possible to modify i(ω) by introducing a different weighting coefficient for k. Assuming equal self-inductance for both transmitting and receiving coils, the finite element analysis results yield the following values for ki(ω):

$$K_i(\omega) = \frac{\int_{\Omega_{coil2}} A_i(\omega)\cdot J_2 d\Omega}{\int_{\Omega coil1} A_i(\omega)\cdot J_1 d\Omega} \tag{8}$$

The given equation involves the dislocation coil ($A_i(\omega)$), the unit vector of current parallel to the receiver (J1), and the receiver coil (J2). It is important to note that $A_i(\omega)$ implicitly depends on the weighting coefficient. To solve this optimization problem using μ GA [9-10], we employed a population size of 5 individuals and conducted evolution for 400 generations.

Table 1

Characteristics of coils wound on both sides

Strand radius	0.30mm
Number of strands	200
Number of turns	3parallelsx1l5turns
Relative permeability of magnetic core	2000
Driving frequency	85kHz
Lateral misalignment(x-axis)	300mm

Forward misalignment(y-axis)	60mm
Air gap length	70+30(-15)mm

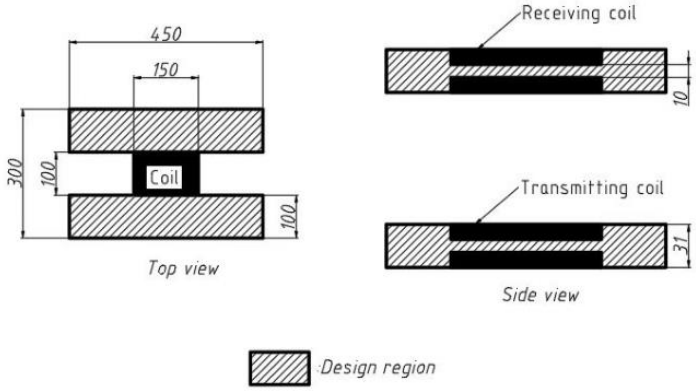

Fig. 2. Optimization model

5. Optimization results and experimental validation

5.1 Optimization results

The optimal model of the double-winding wireless power transfer (WPT) device for electric vehicles is illustrated in Fig. 2, while the coil parameters are summarized in Table 1. To achieve mirror symmetry in both x and z directions, as depicted in Fig. 3, a total of 196 Gaussian functions are uniformly distributed within one-quarter section of the transmitting coil domain to ensure comprehensive coverage. Each Gaussian function represents a sphere with radius sigma located at Xi (i = 1,2,... , N). Although it is relatively straightforward to restrict the lateral displacement using wheel plugs for electric vehicles, we present the optimal model of the bidirectional double-winding WPT device for forward-moving electric vehicles in Fig. 2 along with detailed coil parameters listed in Table 1.

In order to establish mirror symmetry between transmitting and receiving coils along x and z directions, we deploy a uniform distribution of 196 Gaussian functions within one-quarter section of the transmitting coil domain as shown in Fig. 3. These Gaussian functions provide support coverage by placing spheres with radius sigma at specific locations on dislocations along x-axis (y-axis). However, limiting transverse dislocation (x-axis) poses challenges due to stricter tolerance requirements. Therefore, we consider lateral dislocation based on equation (7). Since lateral deviation necessitates precise tolerances, three different deviations are considered: namely, 0 mm, 150 mm and 300 mm corresponding to i =1 ,2 ,3 respectively according to equation (7). Additionally, optimization was conducted to verify the effectiveness of robust optimization.

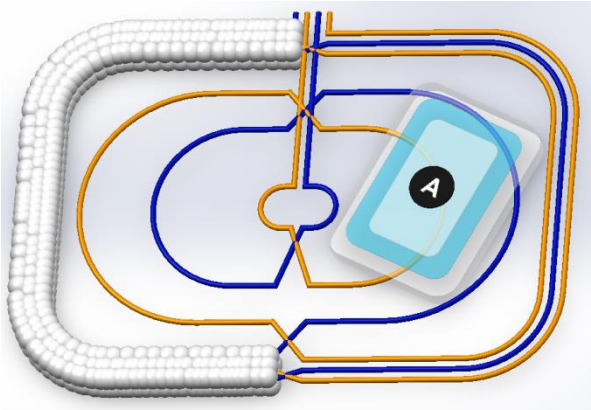

Fig. 3. Distribution of Gaussian functions

We conducted a comparison between the square-coil structure and various other structures. The considered coupler structures are commonly utilized in EV charging systems nowadays, namely rectangular-rectangle (Rec-Rec), double (DD-DD), double pole (BP-BP), and round (Circ-Circ) with ferrite plates, as depicted in Fig. 4. In terms of the ferrite plate, the coil primarily generates a magnetic field on one side while significantly reducing it on the opposite side of the pad. The DD coil (Fig. 4a) and BP coil (Fig. 4b) consist of two interconnected opposing directions. These sub coils effectively minimize transverse leakage flux by facilitating flux transfer between each other.

The overall design of the bipolar coil (BP) (Fig. 4b) closely resembles that of the DD coil which comprises two coils with minimal overlap. The extent of this overlap (O as indicated in Fig. 4b calculated to counter or significantly diminish any mutual influence between the two sub coils forming the BP structure. In this particular arrangement, both sub coils function independently as magnetically decoupled coils.

The circular coil (as depicted in Fig. 4d) is widely utilized in WPT systems, particularly for static charging applications. The outcomes (illustrated in Fig. 5) are presented within the x-axis and y-axis intervals, which correspond to a range of 154% size of the coil.

As the displacement increases, the k values of each topology decrease, albeit in distinct manners. When the two coils are precisely aligned, the Circ-Circ topology yields a maximum k value of 0.245, while the BP-BP topology exhibits a minimal k value when aligned. The simulation results suggest that both DD-DD and BP-BP topology exhibit relatively lower sensitivity to displacement in the "X" with a coupling factor of 50% and coil size k=50.1. By employing both topology, zero coupling is achieved in the "Y" as indicated by the study's 34% discovery. These characteristics of low k values and zero coupling factors serve as significant limitations for these topology suitability in dynamic charging applications,

particularly considering that alignment around 50% is required according to standards.

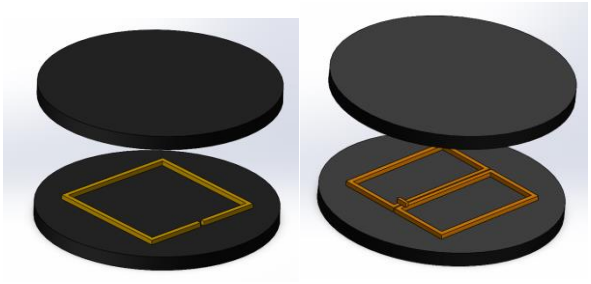

(a) Rec–Rec shaped (b) DD–DD shaped

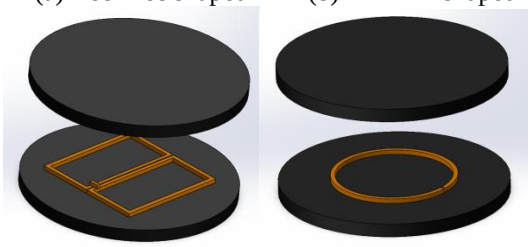

(c) Bp-Bp shaped (d) Circ–Circ shaped

Fig. 4. WPT cores with same ferrite volume

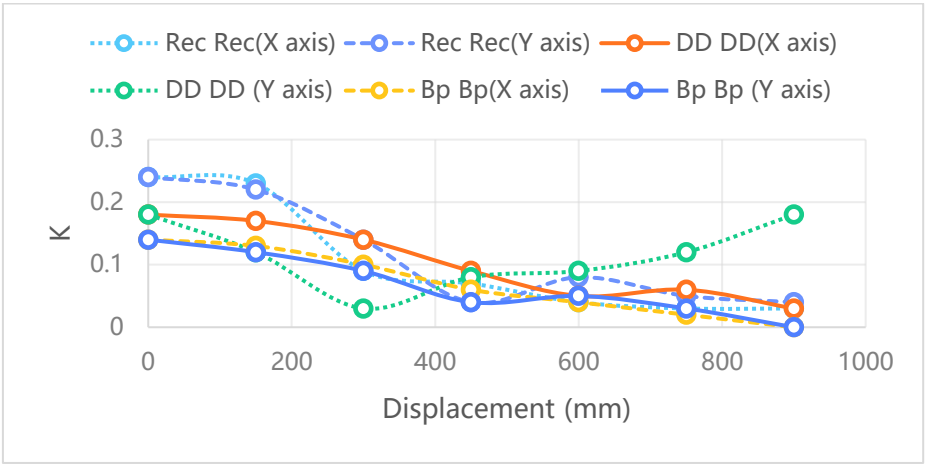

Fig. 5. Coupling factor for different displacement positions

The relationship between the upper nucleus's edge and the lower6, where no flux was detected. we conducted an optimization investigation on the solution dependency in μ GA by modifying five groups generated using a random seed. This analysis is presented through five convergence history scenarios, considering both aligned and misaligned μ GA.

Table 2

Considering misalignment

Generation	Objective function F(w) (Sample 1)	Objective function F(w) (Sample 2)	Objective function F(w) (Sample 3)	Objective function F(w) (Sample 4)
0	0.21	0.14	0.16	0.19
100	0.24	0.24	0.25	0.28
200	0.26	0.28	0.29	0.29
300	0.28	0.30	0.31	0.29
400	0.29	0.32	0.33	0.33

Table 3

Without Considering misalignment

Generation	Objective function F(w) (Sample 1)	Objective function F(w) (Sample 2)	Objective function F(w) (Sample 3)	Objective function F(w) (Sample 4)
0	0	0.04	0.06	0.09
100	0.04	0.04	0.15	0.18
200	0.16	0.18	0.19	0.19
300	0.28	0.22	0.21	0.22
400	0.29	0.32	0.33	0.33

To investigate the dependence of the solution on the initial individual in μGA, we performed an optimization starting with 4 different individual groups by varying random seed generation. The convergence history of μGA with and without error is plotted as shown in Table 2 and Table 3. We can see that the optimization results have almost the same performance because the standard deviations are all less than 1%.

5.2 Experimental validation

Fig. 6. Test bench

It is necessary to conduct an experimental analysis of the electrical characteristics of the coupler in order to verify the accuracy of the finite element model employed. The fabrication process for full-scale coils requires significant time and resources, particularly considering the cost associated with materials such as Litz wire and ferrite. Assuming our system operates within its non-saturation range, we aim to validate previously obtained outcomes by downsizing the coil.

The micro coils were created through a process of downsizing from their actual size, with a 1:10 ratio. This allowed for the validation of previous simulation results using COMSOL software in the lab includes ferrite plates and Litz lines, maintained on level one. It's important while certain dimensions can be uniformly reduced, the thickness of ferritic materials. Each topology was tested at ten different displacement values ranging from 0 (coaxial position) to 50 mm in increments of 5 mm.

This enables us to calculate the mean and standard deviation of this coefficient. To directly compare with the displacement in the numerical model at a 1:1 scale, we multiplied the experimental displacement distance (ranging from 0 to 50 mm) by a scale factor of 10. The normalized self-sensing value obtained from multiplying the distance (0 to 50 mm) by a scale factor of 10 is similar to the numerical calculation, allowing us to focus on comparing coupling factors. Fig. 7 illustrates numerical simulations and experimental measurements for two previously studied coupler topology, along with coupling coefficients derived from displacements (without any dislocation) on the power road axis.

Fig. 7. Comparison between simulated results and measured values of normalized self-inductance

The coupling coefficients obtained through measurements using a reduced-scaling model exhibit strong agreement with those derived from numerical simulations, as depicted in Fig. 8. However, there are disparities between the measured and simulated values, primarily attributed to measurement errors. Moreover, the majority of deviations stem from manual craftsmanship involved in fabricating the coils and couplers, leading to inaccuracies in their precise dimensions. It is worth noting that not all dimensions fully adhere to the employed homotype ratio (1:10). This aspect becomes crucial for use in dynamically charged vehicles due to its tolerance for offset; however, its location on electric roads has yet to be fully determined.

6. Conclusion

In this study, we propose a method for optimizing the shape magnetic core in WPT devices to enhance their coupling efficiency. Our results demonstrate that the optimized core shape significantly improves the coupling coefficient, with Rec Rec shaped cores showing particularly high performance. However, it should be noted that topological advantages may not always be apparent and other shapes may be more suitable for static charging scenarios. Furthermore, our optimized WPT devices perform comparably to conventional ones and future work these findings as well as exploring optimal ferrite plate materials and potential improvements to aluminum shielding integration which can impact parameters such as self-sensing or coupling factors.

Acknowledgments

This work was supported by the Natural Science Foundation of Jiangsu Province University (21KJB460037), Training object of Jiangsu Province "Qinglan Project" (2023), Teaching Innovation Team of Nanjing Institute of Information Technology (2023).

R E F E R E N C E S

[1] Zhang, Ben, et al. "A wireless power transfer system for an autonomous underwater vehicle based on lightweight universal variable ring-shaped magnetic coupling." International Journal of Circuit Theory and Applications 51.6(2023):2654-2673.

[2] Hang, Lu, X. Jiawen, and Y. Ruqiang. "A high-efficient piezoelectric wireless energy transmission system based on magnetic force coupling." Review of Scientific Instruments 94.2(2023).

[3] Geng, Yanfeng, and Z. Zheng. "Wireless Communication for Drilling Using Acoustic Wave Based on MIMO-OFDM." Journal of Circuits, Systems and Computers 32.10(2023).

[4] Vala, Tejas M., V. Rajput, and A. Al-Sumaiti. "Investigating the performance of non-standard characteristics-based over current relays and their optimum coordination in distributed generators connected networks." IET Generation, Transmission & Distribution (2023).

[5] Nonmon, Sanogo Idrissa, et al. "Genetic insights of H9N2 avian influenza viruses circulating in Mali and geographic patterns in Northern and Western Africa." Virus Evolution 1(2024):1.

[6] Shi, Yanyan, et al. "Frequency offset suppression method for wireless power transfer based on nonlinear resonant network." International Journal of Circuit Theory and Applications 51.5(2023):2315-2326.

[7] Li, Xiaodong, T. Lu, and P. Song. "Transmission characteristics of the rough surface scattering channel for wireless ultraviolet communication in a cemented ground scenario." Applied optics 17(2023):62.

[8] Liang, Kaixian, D. Zhu, and J. Liu. "Topology optimization of a spatial compliant parallel mechanism based on constant motion transmission characteristic matrix." Mechanism and Machine Theory: Dynamics of Machine Systems Gears and Power Trand missions Robots and Manipulator Systems Computer-Aided Design Methods (2023).

[9] Zhang, Yanxia, and T. Li. "Fault location for overhead and cable hybrid DC line based on the

energy transmission characteristics." Electric Power Systems Research Aug.(2023):221.
[10] He, Tiefeng, et al. "Analysis and Experiment of Laser Energy Distribution of Laser Wireless Power Transmission Based on a Power sphere Receiver."(2023).
[11] J. Boys, G. Elliott and G. Covic, An appropriate magnetic coupling co-efficient for the design and comparison of ICPT pickups, IEEE Transactions on Power Electronics 22(1) (2007), 333-335.
[12] H. Hasegawa, T. Kashiwagi, Y. Sakamoto and T. Sasakawa, Study of magnet rotor type non-contact transformer, International Journal of Applied magnetic and Mechanics 33(1-2) (2010), 135-144.
[13] M. Budhia, G. Covic and J. Boys, A new IPT magnetic coupler for electric vehicle charging systems, IEEE Industrial Electronics Society (2010), 2487-2492.